Calculation of the electronic structure and the magnetic moments of $Nd_2Fe_{14}B$

1993 J. Phys.: Condens. Matter 5 7859

(http://iopscience.iop.org/0953-8984/5/42/008)

J. Phys.: Condens. Matter 5 (1993) 7859–7870. Printed in the UK

Calculation of the electronic structure and the magnetic moments of $Nd_2Fe_{14}B$

Lars Nordström†§, Börje Johansson† and M S S Brooks‡

† Condensed Matter Theory Group, Department of Physics, University of Uppsala, Box 530, S-751 21 Uppsala, Sweden

‡ Commission of the European Communities, Institute for Transuranium Elements, Postfach 2340, D-7500 Karlsruhe, Federal Republic of Germany

Received 8 April 1993

Abstract. Electronic structure calculations for the permanent magnet material $Nd_2Fe_{14}B$ are presented. The localized 4f spin magnetization density is incorporated in the calculational scheme in an appropriate way. The calculated magnetic moments for the different Fe sites are in good agreement with neutron experiments. It is found that the unusually large local Fe magnetic moments for some of the Fe sites are mainly due to the large distances between the Fe atoms in this structure.

1. Introduction

Since the discovery in the late 60s of the compound $SmCo_5$ and its magnetic properties, the most widely used materials for strong permanent magnets are based on intermetallic compounds of rare earth and transition metal elements. Unfortunately Co is expensive and therefore a lot of effort has been made to find a material as good as $SmCo_5$ based on the cheaper transition metal element Fe. The RFe_5 (R=rare earth element) compounds do not exist and most binary compounds based on Fe and a rare earth element have magnetizations that are too small, coercivities that are too small or critical temperatures that are too low. In 1984 $Nd_2Fe_{14}B$ was discovered [1, 2], a ternary compound that had magnetic properties almost as advantageous as those of $SmCo_5$. The most important effect of the introduction of B is that it makes the Fe inter-distances larger than those in binary compounds, which is favourable for magnetism. This also leads, however, to a rather low Curie temperature [3], 593 K, which is only just enough for applications at room temperature [4].

$Nd_2Fe_{14}B$ crystallizes in a tetragonal structure with 68 atoms or four formula units per unit cell [5–7]. There are two different low-symmetric Nd sites and six inequivalent Fe sites. This complicated structure inevitably makes an electronic structure calculation very difficult and demands a lot of computer power.

At room temperature $Nd_2Fe_{14}B$ has a uniaxial anisotropy with the magnetization along the c axis of the tetragonal lattice. At lower temperature, however, there is a spin reorientation [3], below which the magnetization is along a direction at 30° to the c axis. At low temperature the saturation magnetization is $37.1\mu_B$ per formula unit (f.u.) [3].

§ Present address: Institut für Festkörperforschung, Forschungszentrum Jülich GmbH, Postfach 1913, D-5170 Jülich, Federal Republic of Germany.

0953-8984/93/427859+12$07.50

For theoretical calculations of rare earth transition metal compounds there is a problem arising from the coexistence of localized and itinerant magnetism. Of the earlier first-principles electronic structure calculations on $Nd_2Fe_{14}B$, one has not reported how the 4f magnetization density is treated [8], whether it is ignored or incorporated as a spin polarized core, and another has chosen to treat it in the same way as the itinerant magnetism of the Fe 3d electrons [9]. Here we will use a different approach [10], which we argue is more correct. A brief presentation of some of the present results has already been published [11].

In section 2 we outline this new approach to incorporate the localized magnetism in an electronic structure calculation within density functional theory. The computational details are also given. The results of three different calculations, a paramagnetic calculation, a calculation with zero 4f magnetism and a calculation including the 4f magnetism, are given and discussed in section 3. Finally, the results are summarized in section 4.

2. Method

2.1. The 4f states of neodymium

In electronic structure calculations of crystals within a density functional approach, the charge and magnetization densities are for convenience divided into a valence and a core contribution. The core densities, which are known not to contribute to the bonding and not to differ much from the free atom, might be frozen (as they will be here) or allowed to relax in the iterating procedure (a so-called all-electron approach). For some cases there are ambiguities as regards which electrons it would be better to incorporate as part of the atomic core or among the valence states. This is for instance the case for the 4f electrons in the rare earth elements. While the 4f shell is unfilled in the lanthanide series the 4f wavefunctions are short ranged and the states may generally be considered as localized, i.e. the 4f electrons do not contribute to the bonding of the solid.

In order to describe the cohesive properties of the lanthanide metals, e.g. the equilibrium volumes [12] and cohesive energies [13], the 4f charge density is often taken to be part of the core, whereby fair agreement with experiments is obtained. When magnetic properties are of interest, however, it is clear that the spin magnetization density of the 4f states and its influence on the other valence states ought to be incorporated in the calculation. This has been done successfully for Gd metal with a half-filled 4f shell, by including the 4f states among the valence states and allowing them to spin polarize [14]. For the other elements in the lanthanide series a similar treatment would, however, not be correct. First of all this would inevitably result in very high 4f partial state densities at the Fermi level, which have not been observed in the electronic contribution to the specific heat. Secondly, the 4f magnetic moments are known to retain their atomic-like nature, meaning that there is a coupling between the spin moment and the non-vanishing orbital moment. This property is not at all accounted for in a local spin density treatment. Also, by letting the 4f states form bands there will be serious numerical problems since these bands are very narrow, which gives rise to an extremely slow convergence. Lastly, there will be a bonding contribution from the incompletely filled 4f bands, which is an artifact arising from an overestimation of the hybridization within the local spin density scheme.

In order to circumvent these problems a scheme to treat the 4f magnetization in electronic structure calculations has been proposed [10]. It is based on the assumption that the localized 4f states are better treated when included in the core. In addition to the charge density, a spin density is constructed and incorporated according to the scheme outlined below. This spin density will then influence the valence electrons via the local exchange interaction.

Due to the atomic-like nature of the 4f states, the Russel–Saunders coupling scheme for unfilled shells of free atoms is applicable. This gives an estimation of the spin magnetic moment of the 4f states as

$$\mu_{\text{spin}}^{4f} = 2\mu_B(g_J - 1)J_z \tag{1}$$

where g_J is the Landé factor and J_z is the z component of the total angular momentum $J = L + S$, where L and S are the angular and spin momenta (μ_B is the Bohr magneton). Note that this spin moment differs from the complete spin polarized moment for the light rare earth elements. For example a direct spin polarized core calculation would assume a 4f spin moment of $3.0\mu_B$ for Nd, while the Russel–Saunders value is $2.45\mu_B$. From this spin magnetic moment and the 4f occupation number N^{4f}, we can construct a charge density $n^{4f}(r)$ and a spin magnetization density $m^{4f}(r)$ (both spherically averaged) according to

$$\begin{aligned} n^{4f}(r) &= \tfrac{1}{2}\left(N^{4f} \sum_\sigma |\phi_\sigma^{4f}(r)|^2 + \frac{\mu_{\text{spin}}^{4f}}{\mu_B} \sum_\sigma \sigma |\phi_\sigma^{4f}(r)|^2 \right) \\ m^{4f}(r) &= \tfrac{1}{2}\left(N^{4f} \sum_\sigma \sigma |\phi_\sigma^{4f}(r)|^2 + \frac{\mu_{\text{spin}}^{4f}}{\mu_B} \sum_\sigma |\phi_\sigma^{4f}(r)|^2 \right) \end{aligned} \tag{2}$$

where $\phi_\sigma^{4f}(r)$ is the 4f radial wavefunction solution to the Schrödinger-like equation with a spin split potential and with appropriate boundary conditions. $\sigma = \pm 1$ denotes the different spin states.

The densities in (2) may be considered as part of a semi-core, since they are allowed to change in the iteration procedure and therefore they are not frozen as the ordinary core density is in the present calculation. However, no significant changes are found to occur in the 4f densities within the iteration loop, which seems to indicate that these densities could be frozen as well.

It is the sums of the different charge and magnetization densities that enter the construction of the local potential within the local spin density approximation (LSDA) to the density functional theory. Hence, the spin magnetization of the 4f electrons acts upon the band electrons via the local exchange potential. Therefore, this scheme provides a parameter free approach to the electronic structure calculation of rare earth systems where both localized and itinerant magnetism coexist, although it is not fully a first-principles method.

In cases where the Russel–Saunders coupling is known to fail, either due to crystal field splittings or low-lying multiplets, a more appropriate spin magnetic moment could be inserted instead of (1), e.g. the value obtained from experiments. Also, to study the effects of the 4f magnetization upon the itinerant magnetization of the valence states, μ_{spin}^{4f} can be employed as a model parameter. This is used in the present case where a calculation with zero 4f spin magnetic moment was also performed. This corresponds to those types of calculation where only the 4f charge density is incorporated in the core.

2.2. *Calculational details*

The effective one-particle problem is solved with the linear muffin tin orbital method in the atomic sphere approximation (LMTO–ASA method) [15]. The exchange and correlation part of the LSDA potential is parametrized according to von Barth and Hedin [16]. Angular momenta up to two on the Nd and Fe sites, and up to one on the B site, were included in the

electronic structure calculations, which gives a matrix dimension of 592. Self-consistency was obtained with $18k$ points in the irreducible part of the Brillouin zone. This is a denser mesh than used in earlier works on similar systems [8, 9, 17], but a calculation with $6k$ points, which are then all highly symmetric points, was found not to be sufficient. The Brillouin zone integration was performed with the tetrahedron method. The sphere radii were chosen to have the ratios 1.43:1:0.87 between the Nd, Fe and B atoms. The calculations were performed at the experimentally determined lattice constants [6].

3. Results

3.1. Paramagnetic calculation

The results of a calculation where the magnetization density is constrained to be zero, i.e. paramagnetic, is firstly discussed. The obtained partial 3d state densities for the six inequivalent Fe sites are shown in figure 1. As can be seen the detailed structure varies between the different sites due to the different environments. However, although the nearest-neighbour coordinations and distances are different for the different sites, the band widths are very similar. This is because the states from the different atoms are strongly mixed in the actual bands. It is noticeable that the partial state density of the j_2 site has a more narrow appearance with most character concentrated in a narrow energy region while j_1 and k_2 have a more smeared out and rather featureless state density. These differences mean that there are large variations of the local 3d state densities $D_d(\varepsilon_F)$ at the Fermi energy. In fact if one constructs a local Stoner product α, i.e.

$$\alpha = I D_d(\varepsilon_F) \tag{3}$$

one finds (table 1) that the Stoner criterion $\alpha > 1$, is only fulfilled for some of the Fe sites. In (3) I is the Fe 3d Stoner integral, which is readily calculated from the 3d wavefunctions [18] and is found to be 24 meV independent of the crystallographic site. The fact that the Fe sites are all magnetic with large magnetic moments in the following spin-polarized calculations is again due to the strong mixing of the different atomic characters in the true bands.

Table 1. The total density of states at the Fermi energy, the electron transfer, the d occupation number and the d partial density of states at the Fermi energy are given per atom for the nine different crystallographic sites. The local Stoner products are also given for the Fe sites. The letters in parentheses refer to the local symmetry and correspond to the notations of Herbst *et al* [5].

Site	$D(\varepsilon_F)$	q	n_d	$D_d(\varepsilon_F)$	$I D_d(\varepsilon_F)$
Nd(f)	0.48	−0.47	1.91	0.28	—
Nd(g)	0.55	−0.26	1.81	0.32	—
Fe(c)	3.34	0.14	6.41	3.22	1.42
Fe(k_1)	2.80	0.02	6.46	2.70	1.19
Fe(k_2)	1.82	0.00	6.45	1.72	0.76
Fe(j_1)	1.94	0.06	6.45	1.82	0.81
Fe(j_2)	3.27	0.15	6.47	3.18	1.41
Fe(e)	3.13	−0.05	6.44	3.00	1.32
B(g)	0.12	0.09	—	—	—

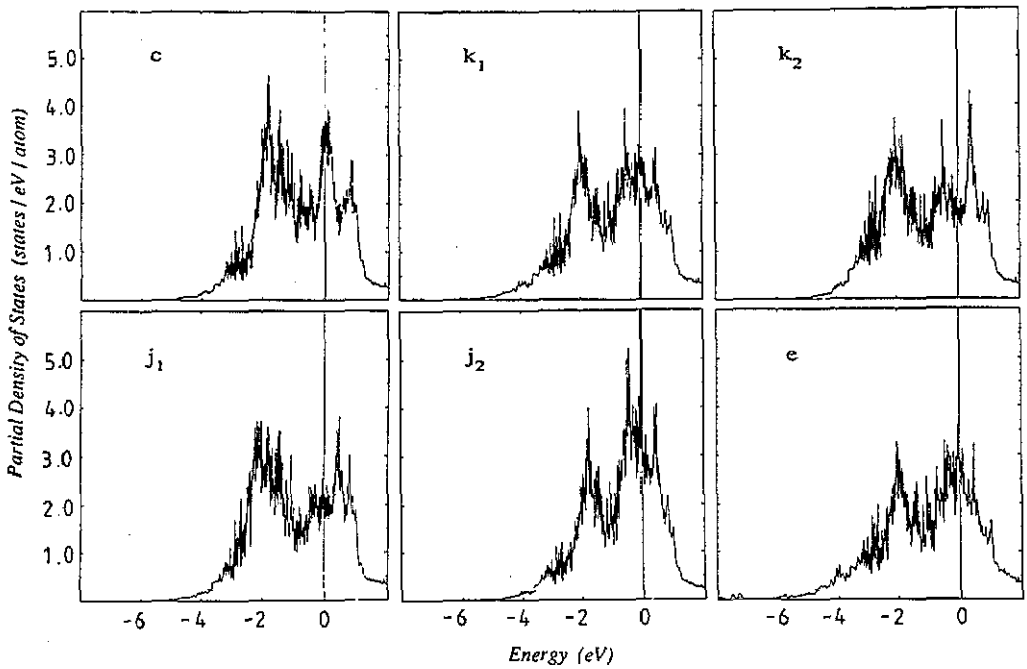

Figure 1. The paramagnetic partial 3d state densities for the six inequivalent Fe sites in $Nd_2Fe_{14}B$. The Fermi energy is situated at zero energy and marked with a vertical line.

The effects of the non-Fe constituents on the Fe 3d states are firstly the ordinary hybridization with the rare earth 5d states, which has been discussed in great detail elsewhere [10, 19]. This brings some Fe 3d states up to the predominantly 5d bands a few electron volts above the Fermi level, and at the same time brings down some 5d character to the Fe 3d bands. This hybridization effectively gives an opposite conduction band spin magnetization on the Fe and Nd sites. Secondly, the presence of the B 2s states in a region 7–8 eV below the Fermi energy will bring a small amount of Fe states down to that region. This can be observed for the e and k_1 partial state densities in figure 1, where there is spectral weight at low energy. That this is most pronounced for the e and k_1 Fe sites correlates well with the fact that these two Fe sites are closest to the B atoms within the crystal.

As regards charge transfers, they are found to be small (table 1), as is expected for calculations for metallic states with reasonable choices of atomic spheres. From the charge transfers obtained it can perhaps be argued that the Nd sphere has been chosen to be somewhat too small.

3.2. Spin-polarized calculation

When the valence states are allowed to spin polarize but the 4f moments are still kept frozen to zero, the results in table 2 are obtained. The local magnetic moments on the different Fe sites are found to vary between $1.9\mu_B$/atom and $2.9\mu_B$/atom. It is noticeable that the site j_2 with the largest moment and that, j_1 with the smallest, have the same local symmetry. A comparison between the presently calculated moments and the Stoner products in table 1 shows a clear correlation. This suggests that there are some Fe sites that drive the rest into a magnetic state, and also that they attain the largest moments themselves.

Table 2. The total local magnetic moment, the electron transfer and the d spin partial density of states at the Fermi energy, for a spin polarized calculation without 4f spin magnetization. Also given are the d projected magnetic moments and the d occupation numbers.

Site	m	q	$D_d^+(\epsilon_F)$	$D_d^-(\epsilon_F)$	m_d	n_d
Nd(f)	−0.35	−0.46	0.09	0.24	−0.26	1.81
Nd(g)	−0.38	−0.26	0.12	0.26	−0.29	1.74
Fe(c)	2.26	0.12	1.01	0.68	2.29	6.37
Fe(k_1)	2.31	0.04	0.66	0.51	2.36	6.36
Fe(k_2)	2.09	0.01	1.12	0.44	2.15	6.38
Fe(j_1)	1.83	0.05	1.56	0.54	1.88	6.41
Fe(j_2)	2.90	0.15	0.30	0.48	2.92	6.34
Fe(e)	2.14	−0.01	0.66	0.45	2.18	6.35
B(g)	−0.18	−0.03	—	—	—	—

Besides the local Fe 3d magnetization there is also a more diffuse magnetization. The magnetic moments on the Nd and B sites are both in the opposite direction to the Fe moments. The magnetization of the Fe sp states is found to be small and in the opposite direction to the Fe 3d moments. Taking into account a total 4f magnetic moment of $3.27\mu_B$/atom on the Nd atoms parallel to the Fe 3d moments, the total magnetic moment is calculated to be $37.1\mu_B$/f.u., which is in very good agreement with experiments.

3.3. Model calculation

In order to obtain some insight into the origin of the difference between the calculated local Fe moments, a tentative model calculation will be discussed below. We will here generalize a simplified analysis, used in earlier investigations [10, 19, 20] of the effects of hybridization, to a case with several inequivalent sites for one atom type. An approximative form of the LMTO Hamiltonian matrix is, for a specific k point, given by

$$H_{QQ'}(k) = C_Q\delta_{QQ'} + \Delta_Q^{1/2}S_{QQ'}(k)\Delta_{Q'}^{1/2} \tag{4}$$

where $Q = (R, l, m)$; R labels the atomic positions and l and m are the ordinary azimuthal and magnetic quantum numbers. C_Q and Δ_Q are the band centre and band width LMTO potential parameters and $S_{QQ'}(k)$ are the so-called structure constants, which are potential independent and uniquely given by the crystal structure.

We now neglect all contributions to the matrices except the matrix elements that couple Fe 3d states to each other. Since we are interested in the importance of the crystal structure to the Fe 3d bands we assume that the C and Δ parameters are equal for all the different Fe sites. This can be verified by direct calculation; the parameters vary very little from site to site. Thus from the Fe sublattice, i.e. without hybridization with Nd or B states, the 3d band widths W_T for the different Fe sites T can be estimated as

$$W_T = [12X_T/(2l+1)]^{1/2}\Delta \tag{5}$$

where X_T is defined by

$$X_T = a(l)\sum_R^{\text{crystal}}{}' \left(\frac{s}{|R-R_{T_0}|}\right)^{2(l+l'+1)} = 7000\sum_R^{\text{crystal}}{}' \left(\frac{s}{|R-R_{T_0}|}\right)^{10} \tag{6}$$

and $a(l) = b(l, l)$, where

$$b(l, l') = 4(2l + 1)(2l' + 1)[(2l + 2l')!/(2l)!(2l')!]. \tag{7}$$

In (6) $\boldsymbol{R}_{T_0}$ is one of the atomic positions for atoms at a type T site and s is the average atomic sphere radius. The sum over the crystal is for all Fe positions except that at $\boldsymbol{R}_{T_0}$. As the terms in the sum over the crystal decrease with increasing distance by a power of ten, it is mostly the nearest-neighbour atom sites that decide the size of X_T. Hence, X_T comprises all information about the nearest Fe environment of site type T, such as the number of nearest Fe neighbours etc. The different values are shown in table 3, where it can be seen that the smallest value is found for the j_2 site, which is also known to have the largest nearest-neighbour distance.

Table 3. Calculated values for X_T (see (6)) and $Y_{TT'}$ (see (8)), where T is Fe 3d and T' is Nd 5d or B 2s, for the six different Fe sites.

Site T	$X_T/10^3$	$Y_{T(\mathrm{Nd\,5d})}$	$Y_{T(\mathrm{B\,2s})}$
Fe(c)	18.9	12.6	0.3
Fe(k_1)	19.1	10.4	2.4
Fe(k_2)	21.7	8.0	0.1
Fe(j_1)	20.7	7.8	0.1
Fe(j_2)	17.2	9.6	0.2
Fe(e)	18.9	7.3	5.3

In a very simple picture the magnetic moment is inversely proportional to the band width. Since the band width in turn is found to be proportional to $X_T^{1/2}$ in (5), we chose to plot the local Fe 3d magnetic moments against $X_T^{-1/2}$ in figure 2. The roughly linear dependence, with the largest magnetic moments for the largest $X_T^{-1/2}$ and smallest moments for smallest $X_T^{-1/2}$, reflects the fact that the local magnetic moments by and large are determined by the Fe inter-distances.

The hybridization with Nd 5d and B 2s states might now be reintroduced as a small perturbation. This corresponds to including the corresponding matrix elements in (4). The relevant quantity that appears in the first-order perturbation theory of the hybridization between T–l and T'–l' states is

$$Y_{TT'} = b(l, l') \sum_{\boldsymbol{R}}^{T' \text{ sub-latt.}} \left(\frac{s}{|\boldsymbol{R} - \boldsymbol{R}_{T_0}|} \right)^{2(l+l'+1)} \tag{8}$$

where $b(l, l')$ is given by (7) above and the sum is to be taken over all atomic positions of the T' site, e.g. the Nd or the B sublattices. In the same way as X above, Y comprises the data concerning the local environment. In table 3 these quantities are collected for the 3d states of the different Fe types with both the Nd 5d and B 2s states. Here it can be seen that the hybridization with the Nd 5d states is almost equally strong for all Fe sites, but slightly stronger for the c sites and weakest for the e sites. The hybridization strength with the B 2s states vanishes for all but the e and k_1 sites, which is consistent with the earlier observations in the plots of the 3d partial states densities for those sites.

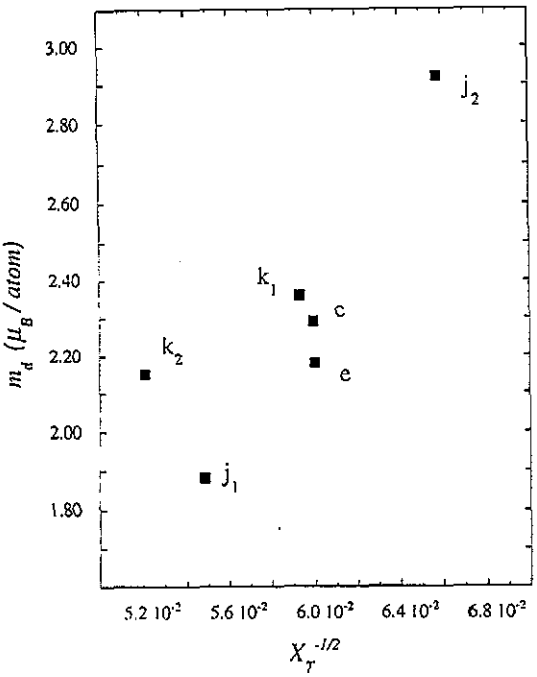

Figure 2. The local Fe 3d spin magnetic moments, obtained from a spin polarized calculation where the Nd 4f moment is zero, are plotted against the local $X^{-1/2}$ for the six inequivalent Fe sites.

3.4. Spin-polarized calculation including 4f magnetization density

Finally the results from a full calculation including the magnetization of the Nd 4f states are presented. With a 4f spin magnetic moment of $2.45\mu_B$/atom and a 4f occupation number of three, charge and magnetization densities are constructed according to (2). These densities are then included in a self-consistent LSDA calculation. The obtained partial state densities are shown in figure 3, and the local magnetic moments are compiled together with other results in table 4. Now the total magnetic moment is $38.1\mu_B$/f.u., which is an enhancement of $1.0\mu_B$/f.u. over the results of the calculation without the 4f magnetization density.

Table 4. As table 2, but for a spin polarized calculation including the Nd 4f spin magnetization density.

Site	m	q	$D_d^+(\varepsilon_F)$	$D_d^-(\varepsilon_F)$	m_d	n_d
Nd(f)	−0.53	−0.49	0.09	0.15	−0.39	1.91
Nd(g)	−0.57	−0.29	0.11	0.15	−0.43	1.83
Fe(c)	2.46	0.11	0.69	0.48	2.50	6.41
Fe(k_1)	2.35	0.03	0.49	0.30	2.41	6.41
Fe(k_2)	2.23	0.01	0.78	0.27	2.30	6.42
Fe(j_1)	2.10	0.05	0.22	0.29	2.16	6.45
Fe(j_2)	2.86	0.15	1.01	0.38	2.89	6.39
Fe(e)	2.15	−0.02	0.43	0.30	2.19	6.40
B(g)	−0.18	0.02	—	—	—	—

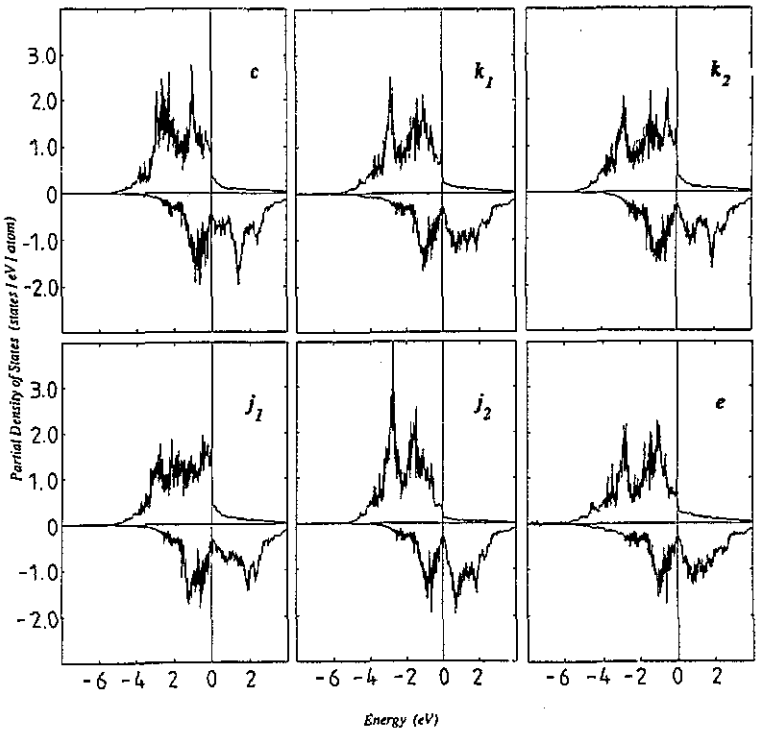

Figure 3. The spin polarized partial 3d state densities for a calculation including the Nd 4f spin magnetization density. The majority (minority) spin states are above (below) the zero axis. The Fermi energy is situated at zero energy and marked with a vertical line.

Although the site resolved partial state densities in figure 3 differ, there are some similarities. For instance they are all very close to complete saturation in the sense that the majority 3d spin states are almost fully occupied. The different degrees of saturation are most clearly seen in the tail-like majority states above the Fermi level. From these it is obvious that the j_2 site is indeed as close to saturation as possible, while the other sites have broader tails and in this respect are further away from saturation. Another similarity can be seen for the minority states, where the Fermi level always appears in a valley of the partial state density.

The inclusion of the 4f magnetization density of course enhances the magnetization of the 5d states, whose magnetic moments are increased by 50%. As concerns the local Fe moments only three seem to be influenced by the inclusion of the 4f magnetization. The magnetic moments of the c, k_2 and j_1 sites are increased while the magnetic moments of the e, k_1 and j_2 sites are almost unaffected. This difference between the influence on the moments of the Fe sites is not directly related to the strength of the hybridization with the Nd 5d states, as can be seen in table 3, where k_1 has one of the strongest hybridizations but its moment is not affected much. Instead these differences can be related to the densities of states at the Fermi level in the calculation without the 4f magnetization. In table 2 one can find the largest state densities at the Fermi level for the majority spins of the c, k_2 and j_1 sites, which are the sites whose moments are found to alter with the inclusion of the 4f magnetization. Hence, in other words, one can regard the Fe sites that have the largest

susceptibilities as being changed with an increase of the effective molecular field, to which the inclusion of the 4f magnetization may be related.

In a similar study of the cubic Laves phase compounds RFe_2 it was found that there was an almost complete cancellation between the increase of the R 5d moments and the increase of the oppositely directed Fe 3d moments with an increase of the R 4f moments [10]. In the present case with several different Fe sites the situation seems to be more complicated. There is still a partial cancellation, but, firstly, as remarked above the change in the Fe moments differs significantly between the sites, and, secondly, the higher Fe concentration in Nd_2Fe_2B makes it more difficult for the Nd 5d moments to cancel the increase of the Fe moments.

4. Summary

In order to understand the origin of the unusually large Fe moments in the ternary compound $Nd_2Fe_{14}B$ several different calculations have been performed. It is found that these magnitudes are to a large extent governed by the pure Fe sublattice and its quite large Fe–Fe inter-distances, and the variation of the different Fe moments is by and large due to the different Fe surroundings. Hence, the Nd and B atoms play only a minor role in the Fe magnetization.

To take into account the presence of the localized Nd 4f magnetization, a newly suggested calculational scheme [10] was used. However, when comparing the total magnetic moments from this calculation on the one hand, and from a calculation without the 4f magnetization on the other, with the experimentally measured value [3], it is found that the latter theoretical value agrees perfectly while the former is too large by $1\mu_B$. However, below the spin reorientation temperature, there are indications of a non-collinear arrangement [21] of the Nd and Fe moments. This means that our calculation, which assumes collinear moments, slightly overestimates the total magnetic moments. A full treatment [22] of this non-collinearity is out of reach for this complicated compound, but a simpler way to estimate the influence of the non-collinearity of the Nd and Fe moments would be to reduce the 4f spin moments, which to some extent should mimic the loss of coupling between these moments.

The obtained local magnetic moments from this calculation are compared with those of earlier calculations [8,9] and neutron scattering experiments [21,23] in table 5. A comparison with the results of a low-temperature neutron experiment [21] shows that the size ordering of the Fe moments is well reproduced but also that the absolute values are in fair agreement with the experimental data. There is a deviation for the Nd moments, but this is likely to be due to the possible non-collinearity of the Nd and Fe moments. Since the concentration of the Nd atoms is much smaller than that of Fe, the effect has to be larger on the Nd moments.

When comparing our calculated moments with those of earlier calculations, a consistency is found with those calculated by Jaswal [8], but larger deviations are found for the results of Gu and Ching [9]. The small differences between the present values and those of [8] is not surprising, since there are slight differences in the computational details. Besides the fact that Jaswal did not include the 4f magnetization density in the same way, he used another choice of sphere radii and fewer k points in the irreducible part of the Brillouin zone. In the calculation of Gu and Ching on the other hand, where the 4f states were included among the conduction states, a wrong sign for the spin magnetic moments on both the Nd and the B sites was obtained. Also, a magnetic moment of $3.4\mu_B$ was obtained for

Table 5. Local magnetic moments on the various crystallographic sites. The present calculation is with a 4f spin moment, and for the Nd atoms the total Nd 4f moment, $3.27\mu_B$, is added to the valence electron contribution. All moments are in units of Bohr magnetons (μ_B).

	Theory			Experiment	
Site	Present	[9]	[8]	[21]	[23]
Nd(f)	2.74	3.01[a]	−0.55[b]	2.30[c]	2.3[c]
Nd(g)	2.70	3.04[a]	−0.52[b]	2.25[c]	3.2[c]
Fe(c)	2.45	2.97	2.59	2.75	2.2
Fe(k_1)	2.35	2.15	2.15	2.60	2.4
Fe(k_2)	2.23	2.28	2.18	2.60	2.4
Fe(j_1)	2.10	2.48	2.12	2.30	2.7
Fe(j_2)	2.86	3.40	2.74	2.85	3.5
Fe(e)	2.15	1.99	2.13	2.10	1.1
B(g)	−0.18	0.36	−0.20	—	—

[a] Includes only the 4f spin moment.
[b] Conduction electron contribution to the magnetic moment.
[c] Consists mainly of the total 4f moment.

the j_2 site, which is larger than one can obtain with a reasonable 3d occupation number. In fact, we believe that the moment of $2.9\mu_B$ obtained in the present calculation is as large as an Fe spin magnetic moment can become within a metal.

Acknowledgments

Dr Jean Rebizant is gratefully acknowledged for his help with the crystal structure data. Lars Nordström and Börje Johansson are both thankful for financial support from the Swedish Natural Science Research Council. The calculations were performed at the Swedish National Supercomputer Centre (NSC) in Linköping under a grant from the Swedish Natural Science Research Council.

References

[1] Sagawa M, Fujimora S, Yamamoto H, Matsuura Y and Hiraga K 1984 *J. Appl. Phys.* **55** 2083
[2] Croat J J, Herbst J F, Lee R W and Pinkerton F E 1984 *J. Appl. Phys.* **55** 2078
[3] Givord D, Li H S and Perrier de la Bathie R 1984 *Solid State Commun.* **51** 857
[4] Buschow K H J 1988 *Ferromagnetic Materials* vol 4, ed E P Wohlfarth and K H J Buschow (Amsterdam: North-Holland) p 1
[5] Herbst J F, Croat J J, Pinkerton F E and Yelon W B 1984 *Phys. Rev.* B **29** 4176
[6] Shoemaker C B, Shoemaker D P and Fruchart R 1984 *Acta Crystallogr.* C **40** 1665
[7] Givord D, Li H S and Moreau J M 1984 *Solid State Commun.* **50** 497
[8] Jaswal S S 1990 *Phys. Rev.* B **41** 9697
[9] Gu Z Q and Ching W Y 1987 *Phys. Rev.* B **36** 8530
[10] Brooks M S S, Nordström L and Johansson B 1991 *J. Phys.: Condens. Matter* **3** 2357
[11] Nordström L, Brooks M S S and Johansson B 1991 *J. Appl. Phys.* **69** 5708
[12] Min B I, Jansen H J F, Oguchi T and Freeman A J 1986 *J. Magn. Magn. Mater.* **61** 139
[13] Eriksson O, Brooks M S S and Johansson B 1990 *J. Less-Common Met.* **158** 207
[14] Sticht J and Kübler J 1985 *Solid State Commun.* **53** 529
[15] Andersen O K 1975 *Phys. Rev.* B **12** 3060
[16] von Barth U and Hedin L 1972 *J. Phys. C: Solid State Phys.* **5** 1629

[17] Coehoorn R 1990 *Supermagnets, Hard Magnetic Materials (NATO-ASI Lecture Notes)* ed G J Long and F Grandjean (Dordrecht: Klüwer)
[18] Gunnarsson O 1976 *J. Phys. F: Met. Phys.* **6** 587
[19] Brooks M S S, Eriksson O and Johansson B 1989 *J. Phys.: Condens. Matter* **1** 5681
[20] Andersen O K, Klose W and Nohl H 1978 *Phys. Rev.* B **17** 1209
[21] Givord D, Li H S and Tasset F 1985 *J. Appl. Phys.* **57** 4100
[22] Kübler J, Höck K-H, Sticht J and Williams A R 1988 *J. Phys. F: Met. Phys.* **18** 469
[23] Herbst J F, Croat J J and Yelon W B 1985 *J. Appl. Phys.* **57** 4086